Journal of The Electrochemical Society, **153** (8) G734-G737 (2006)
0013-4651/2006/153(8)/G734/4/$20.00 © The Electrochemical Society

GaN Light-Emitting Triodes for High-Efficiency Hole Injection

Jong Kyu Kim,[a] E. Fred Schubert,[a,*,z] Jaehee Cho,[b] Cheolsoo Sone,[b] J. Y. Lin,[c] H. X. Jiang,[c] and J. M. Zavada[d]

[a]*Department of Electrical, Computer, and Systems Engineering, Rensselaer Polytechnic Institute, Troy, New York 12180, USA*
[b]*Photonics Program Team, Samsung Advanced Institute of Technology, Suwon 440-600, South Korea*
[c]*Department of Physics, Kansas State University, Manhattan, Kansas 66506, USA*
[d]*U.S. Army Research Office, Research Triangle Park, North Carolina 27709, USA*

A new type of light-emitting device, the light-emitting triode (LET) is demonstrated to have enhanced hole-injection efficiency. The LET has an additional anode to accelerate carriers in the lateral direction by means of an electric field between the two anodes. Theoretical calculations reveal that the lateral electric field provides additional energy to carriers, thereby allowing them to overcome barriers and increasing the carrier injection efficiency into the active region. It is experimentally shown that the light-output power of the LET increases with increasing negative bias to the additional anode, which is fully consistent with the expectation.
© 2006 The Electrochemical Society. [DOI: 10.1149/1.2204873] All rights reserved.

Manuscript received January 16, 2006. Available electronically June 5, 2006.

AlGaN-based ultraviolet (UV) light-emitting diodes (LEDs) are attracting much attention for applications such as chemical and biological detection systems, water and air sterilization, and as a primary light source for phosphor-based white LEDs.[1-3] Although UV LEDs are already commercially available, highly efficient UV LEDs are still difficult to fabricate. Improvement of the efficiency is one of the most important challenges especially for deep UV LEDs ($\lambda < 340$ nm) which have very low internal quantum efficiency. In AlGaN-based UV LEDs, an electron-blocking layer (EBL) is frequently inserted between the p-type cladding layer and the active region. The EBL has the purpose of preventing electron overflow from the active region, and hence, confining electrons to the active region. Figure 1a shows a schematic band diagram of a UV LED with an EBL on a multiple quantum well (MQW) active region. The EBL does not impede hole injection into the active region, if the EBL is heavily p-doped. However, AlGaN with high Al content generally lacks high p-type doping capability which is caused by the high acceptor activation energy of >200 meV. If the EBL is undoped or low p-doped, it will not only block electrons from escaping the active region but also hinder the injection of holes into the active region by the potential barrier, as shown in the Fig. 1a. The tunneling probability of holes through the EBL is low due to a high potential barrier as well as the heavy mass of holes in GaN ($m_h^* = 0.80 \times m_e$) and AlN ($m_h^* = 3.53 \times m_e$). This limits the hole injection efficiency into the active region, and hence internal quantum efficiency.

To overcome the lack of p-type conductivity in bulk films, Mg doped $Al_xGa_{1-x}N$/GaN superlattices (SLs) have been proposed and demonstrated to have a doping efficiency that is 10 times higher than that of bulk p-type GaN.[4,5] The enhancement of carrier transport has been verified in lateral direction, i.e., parallel to the SLs planes. However, carrier transport along the perpendicular direction through p-n junction, which is required in typical light-emitting devices, is less efficient than along the lateral direction because most of the holes ionized from the acceptors are localized inside the quantum wells which are clad by potential barriers as high as 100 to 400 meV.[6] The hindrance of carriers in overcoming the barrier results in a low injection efficiency of carriers in the active region, leading to poor internal quantum efficiency of LEDs. Figure 1b shows a schematic band diagram of an LED with p-type SLs on top of the MQW active region. A schematic description of electron and hole transport in the LED structure is also shown. Efficient injection of holes into the active region of a LED is required for high radiative efficiency. For inefficient hole injection into the active region, electrons will diffuse through the active region into the p-type confinement layer, where nonradiative recombination is likely.

The light-emitting triode (LET) has been motivated by the problem of low injection efficiency in LEDs having a p-type superlattice in the confinement region.[7-9] Schematic sketches of the LED and LET are shown in Fig. 2a and b, respectively. Radiative recombination in active region is strongly required for high-efficiency light-emitting devices. In LEDs, however, nonradiative recombination occurs in p-type confinement region due to an inefficient hole injection over the potential barrier, either by EBL or SLs. The LET is similar to a conventional LED with one important difference: The LET has three terminals, two of which are p-type terminals, anode 1 and anode 2, and one of which is an n-type terminal, cathode, as shown in Fig. 2b. The fundamental operating principle of the LET is as follows. We assume that the cathode is grounded and the two anodes are both biased at a different level. As a result, a current will flow laterally from one anode to the other anode. In the process, the holes will be accelerated, gain a higher energy, and, hence, be able to overcome the potential barrier by either EBL or SLs and be injected into the active region more easily as compared to a device with one anode. Thus, the LET structure is a promising new structure with potential advantages for devices that have SLs in the p-type confinement region as well as for UV devices that have an EBL.

Theoretical Calculation

The carrier temperature can be obtained by equating the energy-gain rate by an electric field to the energy-loss rate by optical phonon scattering. Under steady-state conditions, the two rates are identical, i.e.

$$\left.\frac{dE}{dt}\right|_{\text{electric field}} = \left.\frac{dE}{dt}\right|_{\text{phonon scattering}} \quad [1]$$

with

$$\left.\frac{dE}{dt}\right|_{\text{electric field}} = e\mathcal{E}v = e\mathcal{E}\mu\mathcal{E} = e\mu\mathcal{E}^2 \quad [2]$$

and

$$\left.\frac{dE}{dt}\right|_{\text{phonon scattering}} = \frac{\frac{3}{2}k(T_c - T)}{\tau_e} \quad [3]$$

where μ is the carrier mobility, $\mathcal{E}$ is the electric field, T is the lattice temperature, T_c is the carrier temperature, and τ_e is the optical phonon scattering time. Inserting Eq. 2 and 3 into Eq. 1 and solving for the carrier temperature yields

* Electrochemical Society Active Member.
[z] E-mail: efschubert@rpi.edu

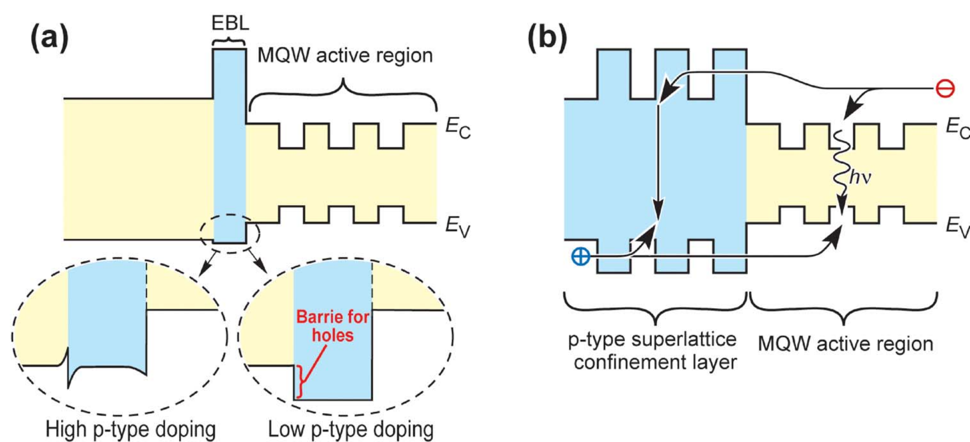

Figure 1. (Color online) (a) Schematic band diagram of a UV LED with electron-blocking layer (EBL) on multiple quantum well (MQW) active region. (b) Schematic band diagram of a UV LED showing electron and hole transport in LED with p-type superlattice confinement region.

$$\Delta T_c = T_c - T = e\mu\mathcal{E}^2\tau_e\frac{2}{3k} \quad [4]$$

Using the Boltzmann distribution, one can calculate the ratio of the carrier concentration at the top of the barrier to the carrier concentration at the bottom of the barrier. This ratio is given by

$$\frac{p_{\text{top}}}{p_{\text{bottom}}} = \exp\left(-\frac{E_{\text{barrier}}}{kT_c}\right) \quad [5]$$

where the height of the barrier is given by E_{barrier}. Assuming that the carrier concentration at the bottom of the barrier is constant, the change in carrier concentration at the top is given by

$$\frac{p_{\text{top}}|_{\text{with field}}}{p_{\text{top}}|_{\text{without field}}} = \exp\left(\frac{E_{\text{barrier}}}{kT} - \frac{E_{\text{barrier}}}{kT_c}\right) \quad [6]$$

This equation directly gives us the expected improvement in the hole injection into the active region of the LET. Figure 3 shows the change in carrier temperature ΔT_c and the ratio of carrier concentration at the top of the barrier $p_{\text{with field}}/p_{\text{without field}}$ as a function of the distance between the two anodes. In the calculation, typical optical phonon scattering time of $\tau_e = 10^{-12}$ s, a p-type GaN hole mobility of 10 $\text{cm}^2/(\text{V s})$, a bias voltage of 5 V, a lattice temperature of T = 300 K, and a barrier height of E_{barrier} = 200 meV are used. Both ΔT_c and $p_{\text{with field}}/p_{\text{without field}}$ increase with decreasing the distance between two anodes, i.e., with increasing electric field.

Note that the ΔT_c and $p_{\text{with field}}/p_{\text{without field}}$ increase rapidly at electric field higher than $\sim 15 \times 10^5$ V/m. For example, one obtains a hole-temperature increase of ΔT_c = 7.7 K, and a corresponding improvement in hole injection by a factor of 1.2 at the distance of d = 5 μm, which gives an electric field of 10^6 V/m. At the distance of d = 1 μm, i.e., electric field of 5×10^6 V/m, the increase of hole-temperature is as high as ΔT_c = 193 K. This corresponds to an improvement in hole injection over the potential barrier by a factor of 20.3. This is a very encouraging theoretical result that motivates the pursuit of the LET. In addition, this calculation suggests a small lateral dimensions between the two anodes in order to get a high electric field that elevates the hole temperature for a reasonable interanode bias range. Scaling down the distance between the anode 1 and anode 2 will afford a reduction in lateral bias. LETs with spiral- and interdigitated-type anodes were designed and fabricated to meet these requirements.

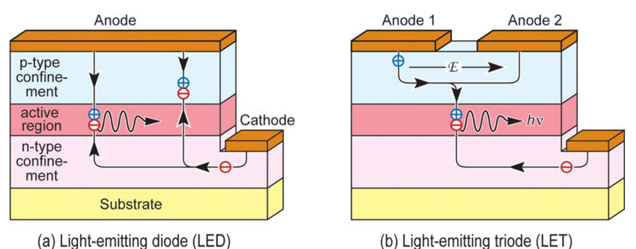

Figure 2. (Color online) (a) Light-emitting diode with nonradiative recombination in p-type confinement region. (b) Light-emitting triode with enhanced hole injection into active region and reduced recombination in p-type confinement layer.

Experimental

LETs were fabricated on two different UV LED wafers. One is a deep UV LED wafer with peak wavelength of λ_{peak} = 305 nm having a p-type $Al_{0.35}Ga_{0.65}N$ EBL. The other is a UV LED wafer with peak wavelength of λ_{peak} = 400 nm having an $Al_{0.15}Ga_{0.85}N$/GaN p-type SL. The 305 nm UV LED structure was grown by metal organic chemical vapor deposition (MOCVD) on c-plane sapphire substrate and consists of a 1 μm thick AlN buffer layer, a 3 μm thick n-type $Al_{0.2}Ga_{0.8}N$ lower cladding layer, a $Al_{0.2}In_{0.03}Ga_{0.77}N/Al_{0.11}In_{0.03}Ga_{0.86}N$ (25/25 Å) double quantum well active region, a 20 nm thick p-type $Al_{0.35}Ga_{0.65}N$ EBL, and a highly doped p-type GaN contact layer. The 400 nm UV LED structure was grown by MOCVD on c-plane sapphire substrate and consists of a 2 μm thick undoped GaN buffer layer, an 3 μm thick

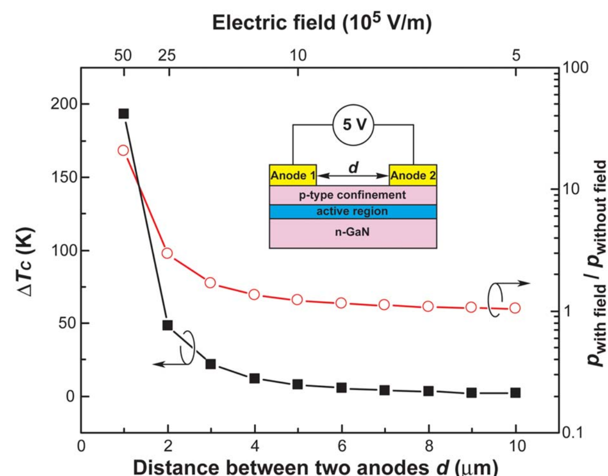

Figure 3. (Color online) The variation in carrier temperature ΔT_c and carrier concentration at the top of the barrier by the bias of 5 V between the two anodes as a function of the distance between the two anodes.

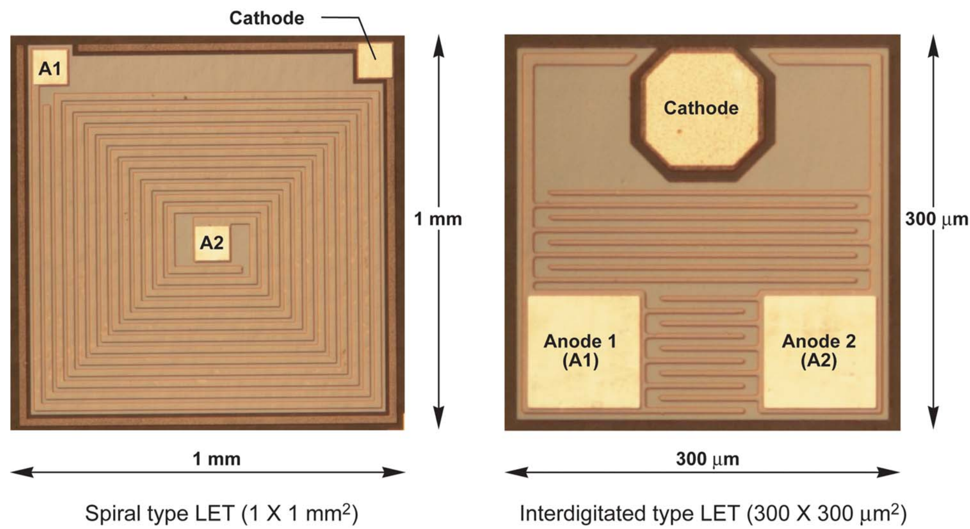

Figure 4. (Color online) Optical micrographs of spiral- and interdigitated-type LETs.

n-type GaN lower cladding layer, six periods of InGaN/GaN MQW active region, a 20 nm thick p-type $Al_{0.15}Ga_{0.85}N$ EBL, 13 periods of p-type $Al_{0.15}Ga_{0.85}N$/GaN (25/50 Å) SLs, and a highly doped p-type GaN contact layer. A 400 nm UV LED wafer without p-type SL was also used for LET fabrication to investigate the effect of the SLs on hole injection efficiency.

LET mesa structures were obtained by standard photolithographic patterning followed by chemically assisted ion-beam etching using Cl_2 and Ar to expose the n-type cladding layer. The n-type ohmic contact was fabricated by electron-beam evaporation of Ti/Al/Ni/Au and annealing at 650°C for 1 min in N_2 ambient. Ni/Au (5/5 nm) ohmic contact layer to p-type GaN was deposited and subsequently annealed at 500°C in an O_2 ambient. Finally, bonding metal was deposited by electron-beam evaporation of Cr/Au (20/500 nm). Figure 4 shows optical micrographs of spiral- and interdigitated-type LETs. The chip dimension is 1 × 1 mm for the spiral-type LET, and 300 × 300 μm for the interdigitated-type LET. The distance between two anodes is 10 μm for the spiral-type LET, and 4 μm for the interdigitated-type LET.

Results and Discussion

The electrical properties of the 305 nm UV LETs are shown in Fig. 5. As a negative bias to anode 2, V_G, increases, the current between anode 1 and cathode increases, as shown in Fig. 5a. Figure 5b shows the transconductance, $G_m = [\partial I_{A1\text{-}C}/\partial V_G]_{VF=constant}$, for

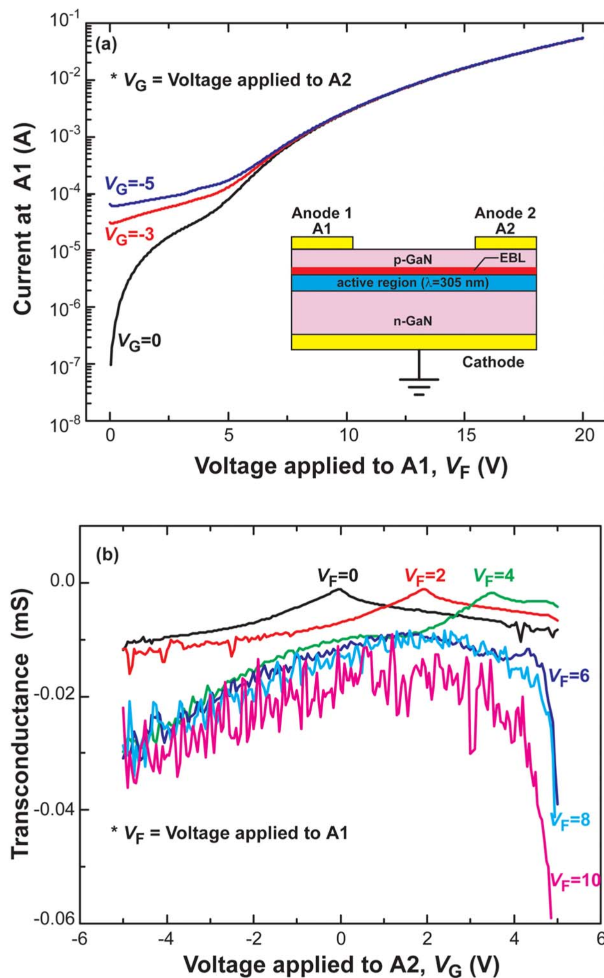

Figure 5. (Color online) (a) Current-voltage characteristics and (b) transconductance, $G_m = [\partial I_{A1\text{-}C}/\partial V_G]_{VF}$ = contant, of the 305 nm UV LET.

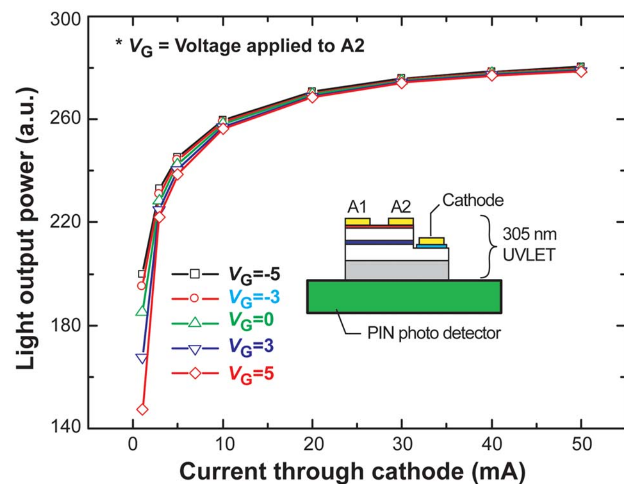

Figure 6. (Color online) The light-output power–vs-current characteristic of the 305 nm UV LETs. The light-output power from the back side of the LET was measured directly on Si PIN photodetector.

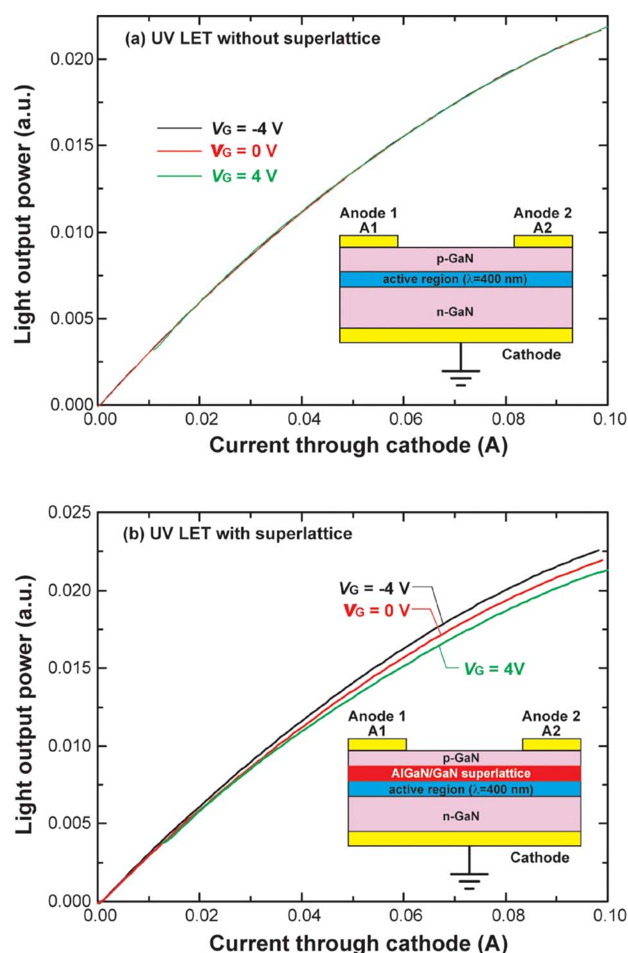

Figure 7. (Color online) The light-output-power–vs-current characteristic of the 400 nm UV LETs (a) without and (b) with AlGaN/GaN SLs.

different voltages between anode 1 and cathode, V_F. As the V_G increases negatively, G_m becomes more negative, which is attributed to an enhanced hole injection efficiency over the potential barrier by the $Al_{0.35}Ga_{0.65}N$ EBL.

The electroluminescence intensity from the back sides of the LETs was measured directly on a large-size $(10 \times 10$ mm$)$ Si PIN photodetector. The light-output–vs-current characteristic of the 305 nm UV LETs is shown in Fig. 6. Inspection of the figure clearly reveals that the light output power depends on the bias to anode 2, V_G, particularly at small forward current values. As the V_G decreases, both the current through cathode and the light-output power increase. This is consistent with the theoretical consideration that a negative bias to the second anode allows carriers to acquire a high kinetic energy thereby enabling them to overcome the barrier for holes, resulting in high hole injection efficiency into the active region that lies beyond the barrier. Although this result was obtained for a UV LET structure with an EBL, it should be reproducible for LET structures employing SLs for the p-type cladding layer.

The light-output-versus-current characteristics of the 400 nm UV LETs without SLs and with AlGaN/GaN SLs are shown in Fig. 7a and b, respectively. No change in light output with V_G is observed for 400 nm UV LET without SLs. However, for the 400 nm UV LET with AlGaN/GaN SLs, the light output power depends on the bias to anode 2, V_G. As the V_G decreases, the light output power increases even though the current through cathode remains constant. This is an important finding and consistent with the expectation that UV LET structure employing SLs as well as employing an EBL showed enhanced light output with increasing negative bias to the additional anode A2. A negative bias to the second anode allows carriers to acquire a high kinetic energy, thereby enabling them to overcome the barrier for holes, resulting in high injection efficiency into the active region that lies beyond the barrier. Furthermore, note that there is no ambiguity at all with respect to the current that flows through the p-n junction. The current measured at the n-type contact must necessarily flow through the p-n junction. Therefore, the results unambiguously confirm the validity of the LET principle.

Conclusion

In conclusion, a new type of light-emitting device, the LET is demonstrated to have enhanced hole injection efficiency. Theoretical calculations reveal that the lateral electric field of 5×10^6 V/m provides an additional energy to holes increasing their temperature by $\Delta T_c = 193$ K, thereby allowing them to overcome potential barriers by either superlattices or electron-blocking layer. This leads to the improvement of hole injection efficiency into the active region by a factor of 20.3. UV LETs ($\lambda_{peak} = 305$ nm) having p-type $Al_{0.35}Ga_{0.65}N$ EBL and UV LETs ($\lambda_{peak} = 400$ nm) having AlGaN/GaN p-type SL are fabricated. It is experimentally shown that the light output power of LETs increases with increasing negative bias to the additional anode. This is consistent with the theoretical consideration that a negative bias to the second anode allows carriers to acquire a high kinetic energy, thereby enabling them to overcome the barrier for holes, resulting in high hole injection efficiency into the active region that lies beyond the barrier.

Acknowledgment

We gratefully acknowledge support from the Army Research Office (ARO), National Science Foundation (NSF), Defense Advanced Research Projects Agency (DARPA), Samsung Advanced Institute of Technology (SAIT), and Crystal IS Corporation.

Rensselaer Polytechnic Institute assisted in meeting the publication costs of this article.

References

1. T. Nishida, N. Kobayashi, and T. Ban, *Appl. Phys. Lett.*, **82**, 1 (2003).
2. S. Shakya, K. H. Kim, and H. X. Jiang, *Appl. Phys. Lett.*, **85**, 142 (2004).
3. J. P. Zhang, X. Hu, Y. Bilenko, J. Deng, A. Lunev, M. S. Shur, R. Gaska, M. Shatalov, J. W. Yang, and M. A. Khan, *Appl. Phys. Lett.*, **85**, 5532 (2004).
4. E. F. Schubert, W. Grieshaber, and I. D. Goepfert, *Appl. Phys. Lett.*, **69**, 3737 (1996).
5. J. K. Kim, E. L. Waldron, Y.-L. Li, T. Gessmann, E. F. Schubert, H. W. Jang, and J.-L. Lee, *Appl. Phys. Lett.*, **84**, 3310 (2004).
6. E. L. Waldon, Y.-L. Li, E. F. Schubert, J. W. Graff, and J. K. Sheu, *Appl. Phys. Lett.*, **83**, 4975 (2003).
7. S. M. Komirenko, K. W. Kim, V. A. Kochelap, and J. M. Zavada, *Solid-State Electron.*, **47**, 169 (2003).
8. S. Luryi, *Appl. Phys. Lett.*, **58**, 1727 (1991).
9. S. M. Komirenko, K. W. Kim, V. A. Kochelap, and J. M. Zavada, *Appl. Phys. Lett.*, **81**, 4616 (2002).